A&A 389, 945–952 (2002)
DOI: 10.1051/0004-6361:20020641

Astronomy & Astrophysics

Radiative transfer in the distorted and irradiated atmospheres of close binary components

A. Peraiah[1] and M. Srinivasa Rao[2]

[1] 57, 4th Cross, 36th Main, BTM 1st Stage, Madiwala-Dollar Scheme, Bangalore 560068, India
e-mail: dspodis@yahoo.com.in
[2] Indian Institute of Astrophysics, Bangalore-560034, India

Received 11 June 2001 / Accepted 5 April 2002

Abstract. We studied the transfer of line radiation in the distorted and expanding atmospheres of close binary components. We assumed that the distortion of the atmosphere is caused by self rotation and tidal force exerted by the presence of the secondary component. The distortion is measured in terms of the ratio of angular velocities at the equator and pole (X), mass ratio of the two components $\frac{m_2}{m_1}$, the ratio of centrifugal force to that of gravity at the equator of the primary (f) and ratio of the equatorial radius of the primary to the distance between the centres of gravity of the two components $\frac{r_e}{R}$. A seventh degree equation is obtained to describe the distorted surface in terms of the above mentioned parameters. We have used $X = 1$ for uniform rotation throughout and used values $f = 0.1$ and 0.5, $\frac{m_2}{m_1} = 1$, and $\frac{r_e}{R} = 0.1$, 0.3, and 0.5. The equation of line transfer is solved in the comoving frame of the expanding atmosphere of the primary using complete redistribution in the line. We used a linear law of velocity of expansion so that the density varies as r^{-3} where r is the radius of the star, satisfying the law of conservation of mass. We set $v_a = 0$ and $v_b = 10$ mtu (mean thermal units) where v_a is the velocity at the surface of the primary with radius $r = a(= 5 \times 10^{11})$ cm and v_b is the velocity at the surface of the extended atmosphere with radius $r = b(= 10^{12})$ cm. We also computed lines in a static atmosphere with density changing as $\rho \sim r^{-1}$. We have considered a primary with an effective temperature T_* and a point source of secondary with three different temperatures T_c equal to 2×10^4 K, 3×10^4 K, and 4×10^4 K.
The maximum change in line fluxes is noticed when the parameters $\frac{r_e}{R}$ and f are changed, while the changes due to $\frac{m_2}{m_1}$ are minimal. The expansion of the atmosphere produces P Cygni type line profiles. The incident radiation from the secondary increases the line fluxes and absorption in the centre of the line is replaced by emission.

Key words. radiative transfer – stars: binaries: close

1. Introduction

The study of close binary systems using light curves, radial velocity curves and changes in the line profiles provide very important information to estimate the vital data about the components. The study of the close binary atmospheres is complicated due to (1) self rotation and (2) tidal effects due to the presence of the companion. These two effects distort the surface of the atmospheres of the components. Further nonuniform temperature distribution in the atmosphere caused by gravity darkening, heating of the atmosphere by the incident radiation from the companion, eclipses, stellar winds and interactions with interstellar gas structures will change the radiation field in the atmospheres of the close binary components. Skulskij (1993) observed the variability of equivalent widths of absorption and emission components of Si II 6347 Å, 6371 Å lines in a study of β Lyrae with CCD spectra.

The changes in the equivalent widths depend on the reflection of the radiation from the companion while the components move in their orbits. The eclipsing binary BE UMa was studied by Ferguson & James (1994) for the reflection effect and cataclysmic variable progenitor characteristics. The reflection effect is due to the close proximity of a late type secondary of a very hot $T \sim 10^5$ K primary sdO star. Several aspects of the reflection effect have been reviewed by Vaz (1985) and Wilson (1990). They found

Send offprint requests to: M. Srinivasa Rao,
e-mail: msrao@iiap.ernet.in

that irradiation from the secondary component will affect the lines and the equivalent widths and that the theoretical bolometric albedos have been found to be in good agreement with observations.

We intend to study the transfer of line radiation in the atmospheres of close binary components that are distorted by self rotation and the tidal effect due to presence of the companion together with the reflection of the light incident from the companion.

In Paper I (Peraiah & Srinivasa Rao 1998) we treated the line transfer problem with reflection effect in an expanding atmosphere while in Paper II (Srinivasa Rao & Peraiah 2000) a dusty, expanding atmosphere was considered. In these two papers we have used a spherical atmosphere without distortion. In this paper we shall consider the atmosphere distorted by self rotation and the tidal effect due to presence of the secondary together with reflection of the incident radiation on the distorted surface from the secondary, considered a point source. The two complexities, i.e. distorted geometry and irradiation from the secondary cannot be treated by the usual symmetric solutions of the transfer equation. The radiation field in the distorted atmosphere consists of two parts (1) self radiation and (2) incident radiation from the secondary component. The first part is treated by using the solution of the transfer equation in spherical symmetry and second part, namely reflected radiation, is calculated using the simple rod model (see Paper I). The contribution of these two radiation fields is used to study the lines formed in the distorted atmosphere. The rod model we used in this paper is simple but not as accurate as a symmetric solution could be (Wing 1962; Sobolev 1963). However, its accuracy can be increased by increasing the number of rays.

2. Calculation of ray segments in the distorted atmosphere

We compute the distorted surface by solving the following seventh degree equation derived by Peraiah (1970). Although better descriptions of the surfaces are available, they do not change our scheme of computation of the source functions in the distorted atmospheres. This is a simple equation to solve and fast solutions can be obtained easily. The equation for the distorted surface is given by

$$\alpha\rho^7 \sin^6\theta + \beta\rho^5 \sin^4\theta + \Big(\gamma \sin^2\theta + J\Big)\rho^3 - \Big(1 - Q\Big)\rho + 1 = 0 \tag{1}$$

where

$$J = Q\Big(3\sin^2\theta\cos\phi - 1\Big) \tag{2}$$

and θ and ϕ are the colatitude and the azimuthal angles respectively. Further, $\rho = \dfrac{r}{r_\mathrm{p}}$, where r and r_p are the radius at any point on the surface and the radius at the pole respectively and

$$\alpha = \frac{f(X-1)^2}{6X^2}\left(\frac{r_\mathrm{p}}{r_\mathrm{e}}\right)^7; \qquad \beta = \frac{f(X-1)^2}{2X^2}\left(\frac{r_\mathrm{p}}{r_\mathrm{e}}\right)^5$$

$$\gamma = \frac{f}{2X^2}\left(\frac{r_\mathrm{p}}{r_\mathrm{e}}\right)^3; \quad Q = \frac{1}{2}\mu\left(\frac{r_\mathrm{p}}{r_\mathrm{e}}\right)^3; \quad \mu = \frac{m_2}{m_1}\left(\frac{r_\mathrm{e}}{R}\right)^3.$$

Here X is the ratio of angular velocities at the equator and pole, f is the ratio of centrifugal to gravity forces at the equator, $\dfrac{m_2}{m_1}$ is the mass ratio of the two components and $\dfrac{r_\mathrm{e}}{R}$ is the ratio of the radius at the equator to the separation between the centres of gravity of the two components. The ratios $\dfrac{r_\mathrm{p}}{r_\mathrm{e}}$ can be obtained from a third degree equation given by

$$\left(\frac{r_\mathrm{e}}{r_\mathrm{p}}\right)^3 - u\left(\frac{r_\mathrm{e}}{r_\mathrm{p}}\right)^2 - \frac{1}{2}\ \mu = 0, \tag{3}$$

where

$$u = 1 + \frac{f\left(X^2 + X + 1\right)}{6X^2} + \mu. \tag{4}$$

Equation (1) is solved for various values of θ and ϕ to obtain the surface for a given set of parameters given the parameters X, $\dfrac{m_2}{m_1}$, f and $\dfrac{r_\mathrm{e}}{R}$ and we always set $X = 1$. The numerical solution is obtained with a starting value of $\dfrac{r}{r_\mathrm{p}} = 1$. Equation (3) is solved by the Newton-Raphson method. These are described in papers of Peraiah (1969, 1970).

We have drawn a schematic diagram in Fig. 1 for the purpose of computing the ray lengths. The points O and B are respectively the centres of the primary and secondary that is supposed to be a point source. The rays such as BA_1, BD, BP, ..., from the secondary (B) are incident on the distorted atmosphere (the surface of which is described by Eq. (1)) at points such as A_1, D, P, ... These points are joined to the centre of the primary O. Further we draw perpendiculars from these points to the axis OB. These perpendiculars meet the rays at the points as shown in the Fig. 1. (1) We need to find the source functions along the rays BA_1, BD, BP, ..., to compute the radiation field in the medium generated by incidence of the light from the secondary. (2) We also need to find the source functions along the perpendiculars such as DJ, PK, SL, ..., to calculate the radiation field along the line of sight and at the observers point at infinity. For this we have to calculate their geometrical lengths and optical depths. The computation of these geometrical lengths is described in Appendix A.

3. Brief description of the model and discussion of the results

We considered an atmosphere of the primary whose radius is twice as large as that of the primary with an inner

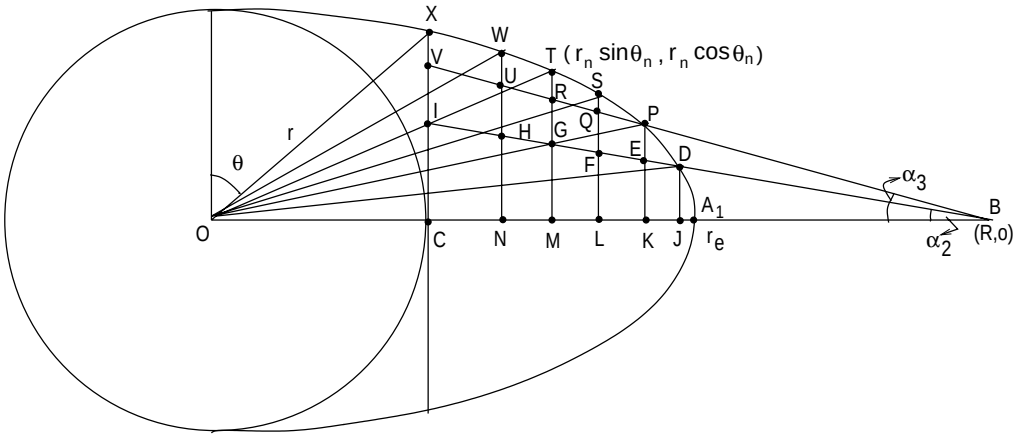

Fig. 1. Schematic diagram of the distorted atmosphere of the component.

radius set to equal to 5×10^{11} cm and the outer radius set to 10^{12} cm. The distortion is considered from the outer radius (10^{12} cm) of the atmosphere. We considered two types of velocity and density laws both of which obey the law of conservation mass, namely $\dot{M} = 4\pi r^2 \rho v$ where $\dot{M}$ is the mass loss rate, ρ is the density, v is the velocity at the radius r. These two laws are (1) $v \sim r$ and $\rho \sim r^{-3}$ and (2) $v \sim r^{-1}$ and $\rho \sim r^{-1}$. We have used a value of 10^{14} cm^{-3} for the electron density for the purpose of calculating the optical depth.

We compute the source functions (S_r) along the rays $BA_1JK \ldots$, $BDEFG \ldots$, $BPQR \ldots$, using the above data and with the help of the rod model which is described in detail in Paper I (see also, Peraiah 2002). The radiation from the secondary component (B) is incident at points such as A_1, D, P, S, ..., on the distorted atmosphere of the primary, and with intensity equal to $\left(\frac{\sigma T_\mathrm{c}^4}{4\pi r_\alpha^2}\right)\cos\alpha$, where σ is the Stefan-Boltzmann constant, T_c is the effective temperature of the secondary (with centre at B), α is the angle made by the ray with the axis OB and r_α corresponds to the ray lengths such as BA_1, BD, BP, ...

The source function (S_s) representing the self radiation is calculated by solving the transfer equations (17) and (18) of Paper I. We employed complete redistribution in the line formed in a scattering medium ($\epsilon = 0$, where ϵ is the probability per scattering that a photon is thermalised by collisional de-excitation). The initial condition at $\tau = \tau_1$ is given in terms of the frequency-integrated Planck function $\left(\frac{\sigma T_*^4}{4\pi}\right)$ where T_* is the effective temperature of the primary (see for example, problem 1.7 of Peraiah 2002).

We have shown the source functions for only 24 rays and in practice we take many more rays into consideration to obtain the desired accuracy, by increasing the the value of n (see Appendix A).

The source function labeled 1 extends all along the axis A_1O while those of the rays with higher numbers continuously get shortened as these latter rays are incident to the atmosphere at angles $\alpha > 0$ and therefore at points on the atmosphere that are progressively towards the centre of the star or shortened lengths R_imp. The ray source functions are maximum at the point of incidence on the atmosphere such as A_1, D, P, ..., that at BA_1 being highest of all. The ray A_1 traverses through the longest path and as the density varies as r^{-3}, the ray encounters denser medium in the interior and consequently has larger number of scatterings. This reduces the source function towards the interior. However the rays whose $\alpha > 0$ travel through smaller paths and hence undergo smaller number of scatterings (also due to the fact that the density changes as r^{-3}) and therefore have enhanced S_r compared to those of the rays whose α are smaller.

In Fig. 2a the two scales on the right- and left-hand sides of the graph are approximately of the same order. Therefore we can distinctly see the three curves S_r, S_s and S, while this is not so in Figs. 2b–d. We cannot distinguish between S_r and S_s. The parameters $\frac{r_\mathrm{e}}{R}$ and f are increased from 0.1 each in Figs. 2a, b to 0.5 in Figs. 2c, d.

This change of parameters produces an increased distorted atmosphere that can see the increase of R_imp by almost 10 times from 4×10^{11} cm in Figs. 2a, b to 4×10^{11} cm in Figs. 2c, d. There is a perceptible change in the self-radiation of the two atmospheres.

Figures 3a–d give the source functions along the rays A_1O, DI, PV, ..., labeled as 1, 2, 3, ..., versus the optical depths along the rays 1, 2, 3, ..., respectively for the corresponding parameters of Figs. 2a–d. The curve labeled 1 represents the source function corresponding to the ray A_1O which is the longest as it is along the axis A_1O ($\cos\alpha = 1$) and the curve labeled 24 corresponds to the source function of the ray with $\alpha = \alpha_\mathrm{max}$ or with minimum value of $\cos\alpha$ ($0 < \alpha < \frac{\pi}{2}$) . We measured the optical depths from the points of incidence of the rays such as A_1, D, P, ... At these points, the source function is maximum for each ray and slowly falls as the optical depth increases along the ray towards the interior of the distorted medium of the atmosphere and reaches maximum.

Figures 4a–d present the line profiles at the observer's point at infinity corresponding to the parameters for which Figs. 2a–d and the 3a–d (see Peraiah 2002, Chap. 8 for

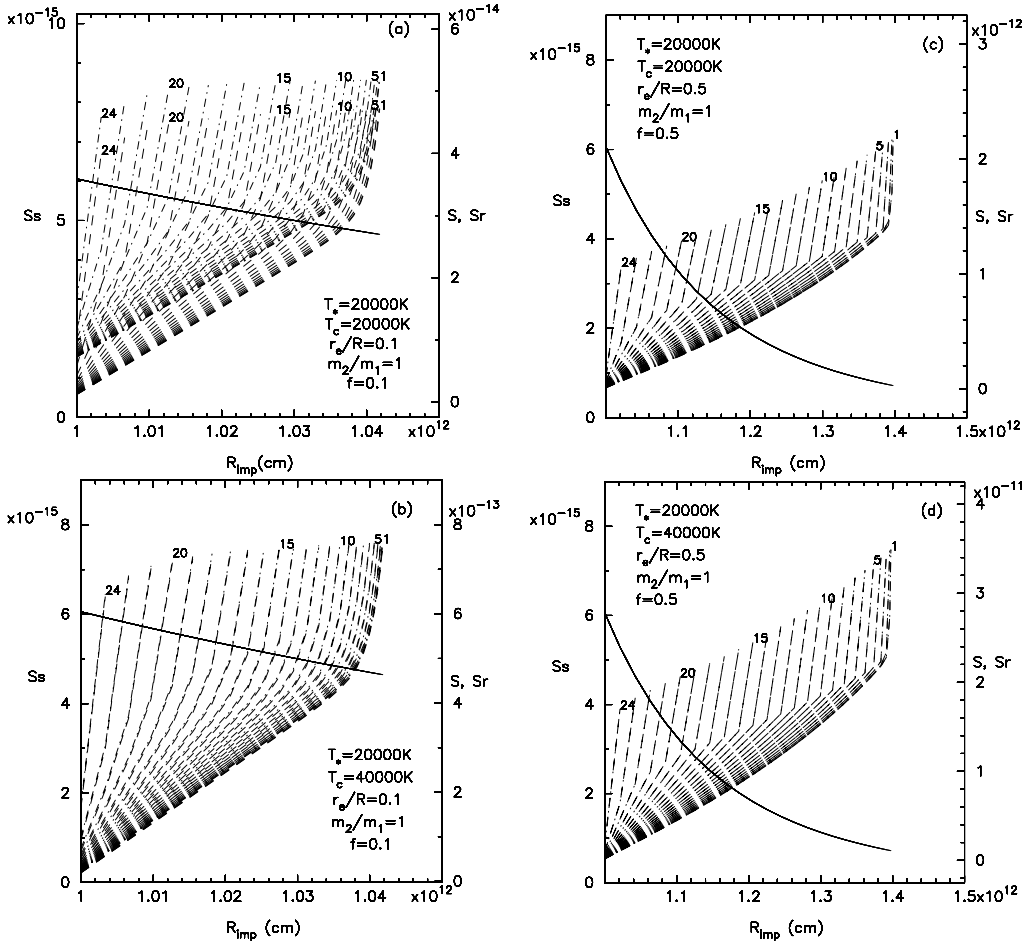

Fig. 2. Source functions along the rays inside the distorted surface with respect to the distances along the axes OA_1. $R_{\rm imp}$ represents the values OA_1, OJ, OK, ... We have given an irradiation proportional to $\left(T_{\rm c}/T_*\right)^4$ where T_* is the temperature of the primary with centres at O and $T_{\rm c}$ is the temperature of the star at B (see Fig. 1). The density varies as r^{-3} The source functions $S_{\rm s}$, for the self radiation are shown through the solid line with the scale given on the left side of the graph while those representing the ray source functions $S_{\rm r}$ are shown by the dashed lines with its scale given on the right side of the graph. The combined source function $S(= S_{\rm s} + S_{\rm r})$ are shown by the dashed dot curves with its scale given on the right side of the graph. The numbers given in these figures such 1, 5, 10, 15, 20, 24 represent the rays such as A_1C, DI, PV, ... The S's are plotted against the distances $R_{\rm imp} = A_1O$, JO, KO, ... The ray corresponding to A_1C is labeled as 1 and that corresponding to DI as 2 and so on.

the procedure) are drawn. The profiles shown by continuous lines are due to the self-radiation whose scale is given on the left side of the graph while the profiles shown by dashed lines are due to the incident radiation and the dashed-dot curves represent the profile due to the combined source function $S = S_{\rm s} + S_{\rm r}$ whose scale is shown on the right side of the graphs. It is interesting that while the profile due to the self radiation is an absorption profile, those due to incident radiation and a combination of self and incident radiation are emission profiles. This suggests that the incident radiation from the secondary adds to the radiation at all frequency points in the line, particularly the centre of the line. The absorption core produced by the self radiation of the star gets more of the incident radiation scattered into the core, making it appear in emission.

Figures 5 and 6 contain three panels each. Panels (a) and (b) give the source function and panel (c) contain the corresponding line profiles. The first panel (a) contains the ray source functions against the total optical depths for rays 1, 6, 12, and 18. The graphs are given for $\dfrac{r_{\rm e}}{R} = 0.1$ and 0.5. The graphs in the (b) panel contain the corresponding source functions S with respect to the $R_{\rm imp}$. The third panel (c) contain the corresponding line profiles along the line of sight. In Fig. 5c contains the profiles in a stationary atmosphere and one obtains symmetric lines. The self radiation produces absorption profiles while the incident radiation produces emission profiles and the combination of the self and incident radiation produces emission profiles. Figure 6 gives the results for an expanding atmosphere with $v_a = 0$ and $v_b = 10$ mtu (mean thermal units) where v_a and v_b are the velocities at the bottom and top of the atmosphere for the velocity law $v \sim r$ and $\rho \sim r^{-3}$.

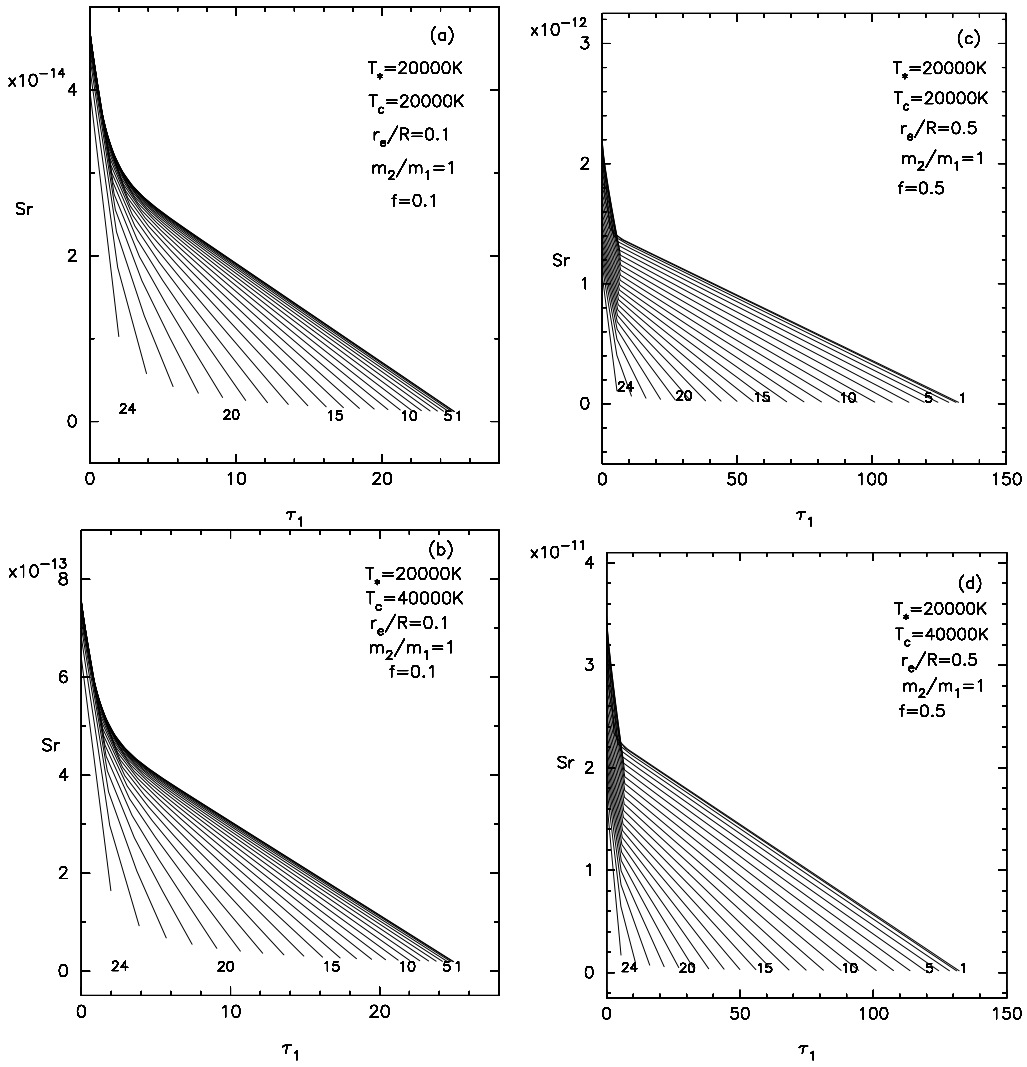

Fig. 3. The source functions are plotted against the optical depths τ_1's measured along the rays such as A_1JKL, ..., DEFG. The curve labeled 1 corresponds to the ray A_1JKL, ..., the curve labeled 2 to the ray DEFG, ...

The profiles due to the self radiation (see Fig. 6c) are almost non-existent and while those due to self and incident radiation are prominent emission lines with P Cygni characteristics. There is a perceptible change in the profiles when the parameter $\frac{r_e}{R}$ is changed from 0.1 to 0.5.

4. Conclusions

We have developed a computational procedure to compute lines formed in the tidally and rotationally distorted atmosphere of the primary component of close binary star, irradiated by the radiation from secondary component. We used a two-level atom approximation with complete redistribution. It is found that the absorption features produced due to self radiation may vanish and emission profiles will appear when the atmosphere is irradiated.

Further, the distortion in the atmosphere increases substantially when the parameters $\frac{r_e}{R}$ and f are increased (compare R_{imp} in Figs. 2a, b with those in Figs. 2c, d). It is necessary to consider the proximity of the secondary and the self rotation of the component in considering the distortion of the atmosphere. We have considered the secondary as a point source in this study. However, we have to study the changes due to the reflection effect on the lines formed and the total light reflected when an extended source of light is considered instead of a point source. This is under study.

Acknowledgements. The authors would like to thank Dr. A. Men'shchikov for suggestions that improved the contents of the paper.

Appendix A:

We need to find the point (or radius of the atmosphere) where the outermost tangent from the point B touches the distorted surface of the atmosphere of the star. Assume that in the case of an unperturbed star

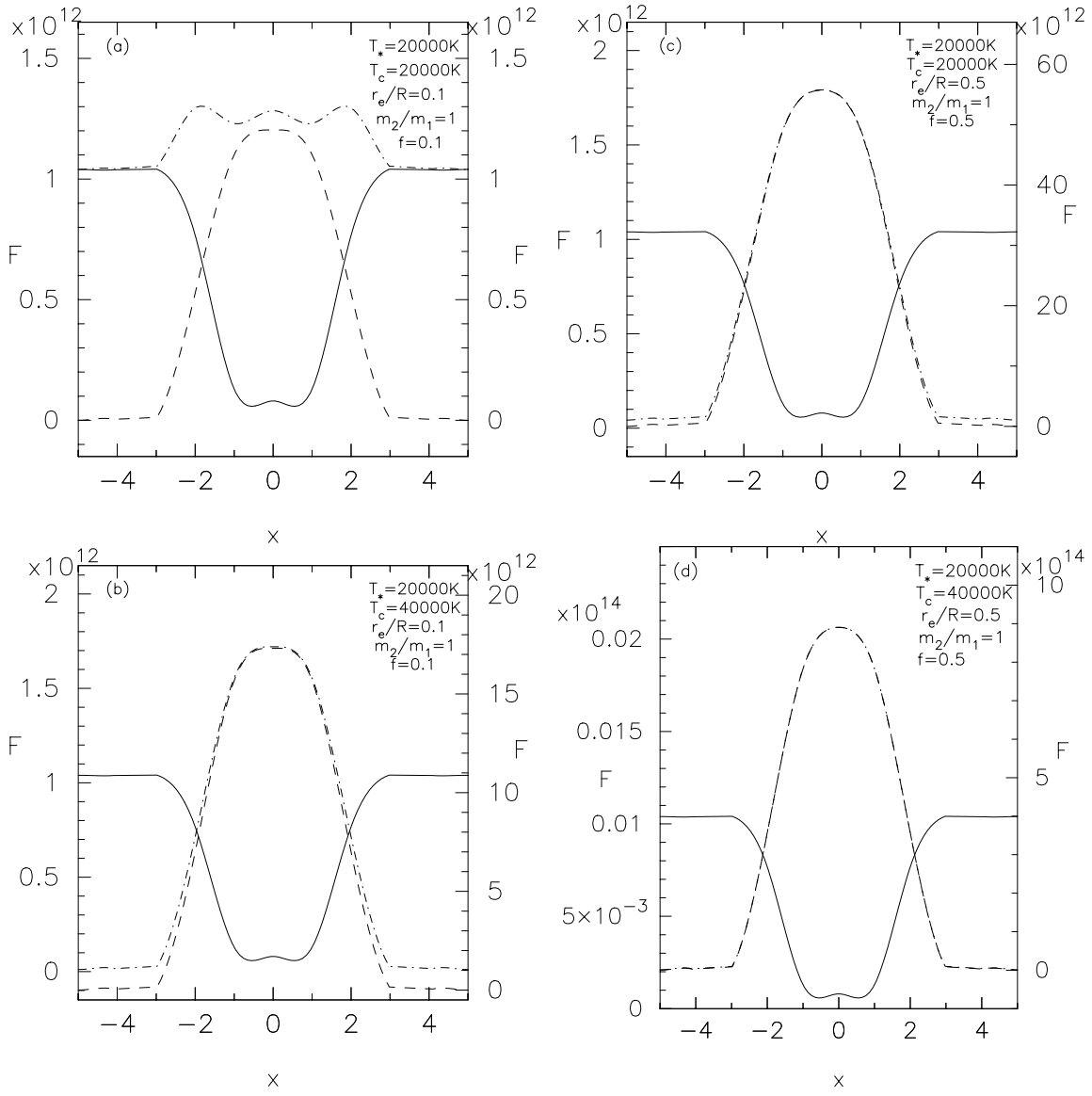

Fig. 4. The flux profiles are plotted against frequency measured in units of Doppler width x, $\left(\text{where } x = \dfrac{(\nu - \nu_0)}{\Delta\nu_{\rm D}},\ \nu \text{ and } \nu_0 \right.$ being the frequencies in the line and at the centre of the line and $\Delta\nu_{\rm D}$ is the Doppler width$\left.\right)$ for $\rho \sim r^{-3}$.

OC $= r_{\rm p}$. Specifying the parameters x, f, $\dfrac{r_{\rm e}}{R}$ and m_2/m_1 and using the Eqs. (1) and (2) we can find the $\theta = \theta_{\rm c}$ where $r_1 \sin\theta_{\rm c} = r_{\rm p}$. This is done by repeatedly solving Eqs. (1) and (2) with small values of θ (by steps of 1°). Now we can divide $(90 - \theta_{\rm c})$ into n intervals and compute the radii r_n to the surface of the distorted reflecting atmosphere. Each radius r_n to the surface can be computed by using $\theta_n = 90 - (n-1)\Delta\theta$, where $\Delta\theta = (90 - \theta_{\rm c})/n$. Let the X-axis coincide with OB and the Y-axis be perpendicular to it. Then the X-coordinates of the point C, N, M, L, K, …, will be $r_1 \sin\theta_1, \ldots, r_{n-1}\sin\theta_{n-1} (= r_{\rm e})$ and the Y-coordinates are all zeros. The general coordinates of any ray which meets the surface are $(r_n \sin\theta_n, r_n \cos\theta_n)$. The X-coordinate of $\rm A_1$ is $r_{n-1}\sin\theta_{n-1}$. Therefore, $\rm BA_1 = R - r_{n-1}\sin\theta_{n-1}$.

Let the angle made by the ray with CB be α, then

$$\tan\alpha_{n-1} = \frac{r_{n-1}\cos\theta_{n-1}}{(R - r_{n-1}\sin\theta_{n-1})}.$$

Similarly,

$$\tan\alpha_n = \frac{r_n \cos\theta_n}{(R - r_n \sin\theta_n)}.$$

If we start with $\theta = 90° = \theta_1$, then $x = r_{\rm e} = r_1 \sin 90 = r$

$y = 0$ (thisisthepoint $\rm A_1$).

θ_2 : $x_2 = r_2 \sin\theta_2$, $y = r_2\cos\theta_2$ $\rm DJ = r_2 \sin\theta_2$

$$\tan\alpha_2 = \frac{\rm DJ}{\rm JB} = \frac{r_2\cos\theta_2}{(R - r_2\sin\theta_2)} = T_2(\text{ say}).$$

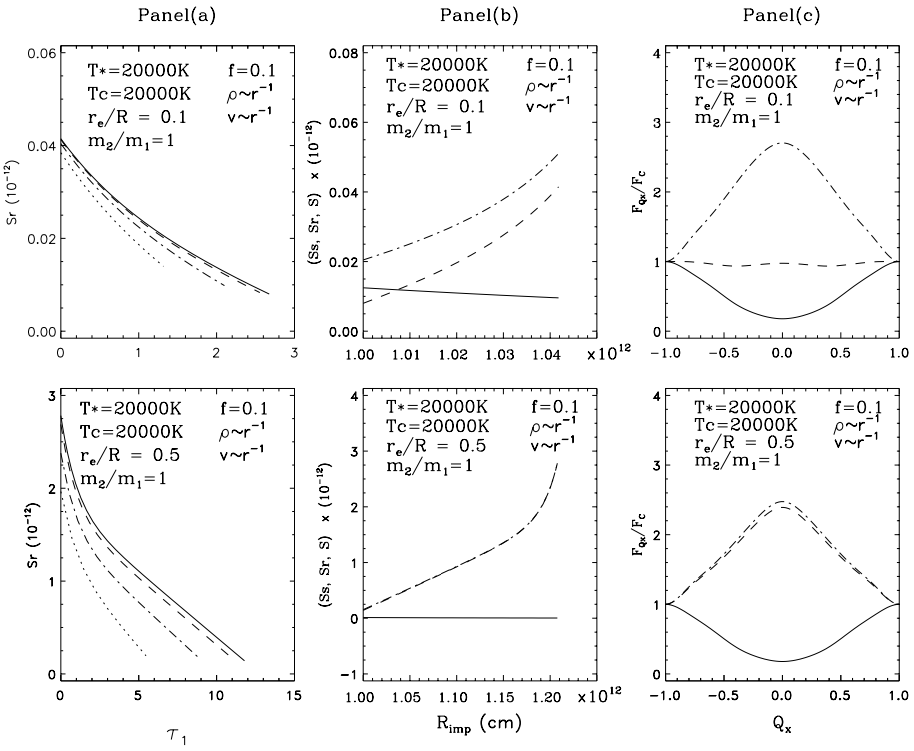

Fig. 5. The ray source functions versus the optical depths along the ray for $\frac{r_e}{R} = 0.1$, 0.5. Continuous line for ray 1, dashed line for ray 6, dashed-dotted for ray 12 and dotted line for ray 18 are given above. Panel **a)** $v_a = 0$, $v_b = 0$, Panel **b)** shows the source functions versus $R_{\rm imp}$ plotted for $\frac{r_e}{R} = 0.1$, 0.5 Source functions for self radiation continuous line (S_s), distorted for different source function dashed line of the distorted atmosphere (S_r), total source function (S) dashed-dot. Panel **c)** shows the normalized fluxes $\frac{F_{Q_x}}{F_c}$ against Q_x where F_c is the flux in the continuum and $Q_x = \frac{x}{x_{\max}}$ (see Fig. 4 for the definition of x). Fluxes due to self radiation are shown by the continuous line, those due to distorted source function by dashed line, and those due to total source function by the dashed dot.

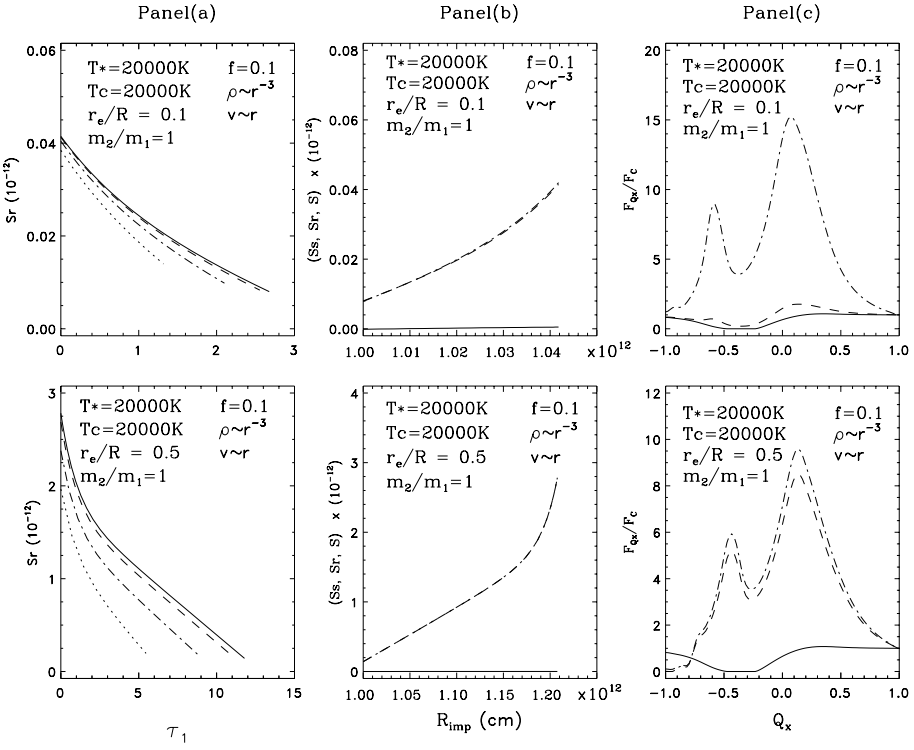

Fig. 6. Same as Fig. 5 but with $v_a = 0$ and $v_b = 10$ mtu (mean thermal units).

From Fig. 1, we have,

$\mathrm{OA_1} = \mathrm{r_e} = \mathrm{r_1}$

$\mathrm{OJ} = \mathrm{r_2}\sin\theta_2$

$\mathrm{OK} = \mathrm{r_3}\sin\theta_3$

$\mathrm{OL} = \mathrm{r_4}\sin\theta_4 \ldots$

$\mathrm{DB}^2 = \mathrm{DJ}^2 + \mathrm{JB}^2 = r_2^2\cos^2\theta_2 + (R - r_2\sin\theta_2)^2$

$\mathrm{EB}^2 = \mathrm{EK}^2 + \mathrm{KB}^2 = (1 + T_2^2)(R - r_3\sin\theta_3)^2$

$\mathrm{FB}^2 = \mathrm{FL}^2 + \mathrm{LB}^2 = (1 + T_2^2)(R - r_4\sin\theta_4)^2 \ldots$

$\mathrm{DJ} = \mathrm{r_2}\cos\theta_2$

$\mathrm{EK} = \mathrm{T_2KB} = \mathrm{T_2(R - OK)} = \mathrm{T_2(R - r_3}\sin\theta_3)$

$\mathrm{FL} = \mathrm{T_2LB} = \mathrm{T_2(R - OL)} = \mathrm{T_2(R - r_4}\sin\theta_4)$

$\mathrm{GM} = \mathrm{T_2MB} = \mathrm{T_2(R - OM)} = \mathrm{T_2(R - r_5}\sin\theta_5) \ldots$

$\mathrm{A_1B} = R - r_\mathrm{e}(= r_1)$

$\mathrm{JB} = R - r_2\sin\theta_2$

$\mathrm{KB} = R - r_3\sin\theta_3$

$\mathrm{LB} = R - r_4\sin\theta_4 \ldots$

$$\tan\alpha_3 = T_3 = \frac{\mathrm{PK}}{\mathrm{KB}} = \frac{r_3\cos\theta_3}{(R - r_3\sin\theta_3)}$$

$\mathrm{PK} = \mathrm{r_3}\cos\theta_3$

$\mathrm{QL} = \mathrm{T_3LB} = \mathrm{T_3(R - r_4}\sin\theta_4)$

$\mathrm{RM} = \mathrm{T_3MB} = \mathrm{T_3(R - r_5}\sin\theta_5)$

$\mathrm{UN} = \mathrm{T_3NB} = \mathrm{T_3(R - r_6}\sin\theta_6) \ldots$

$\mathrm{PB}^2 = \mathrm{PK}^2 + \mathrm{KB}^2 = r_3^2\cos^2\theta_3 + (R - r_3\sin\theta_3)^2$

$\mathrm{QB}^2 = \mathrm{QL}^2 + \mathrm{LB}^2 = (1 + T_3^2)(R - r_4\sin\theta_4)^2$

$\mathrm{RB}^2 = \mathrm{RM}^2 + \mathrm{MB}^2 = (1 + T_3^2)(R - r_5\sin\theta_5)^2.$ (A.1)

We need to know the geometrical length of all the above segments for the computation of the optical depths and source functions along these segments.

References

Ferguson, D. H., & James, T. A. 1994, ApJS, 94, 723

Peraiah, A. 1969, A&A, 3, 163

Peraiah, A. 1970, A&A, 7, 473

Peraiah, A. 2002, An Introduction to Radiative Transfer: Methods and Applications in Astrophysics (Cambridge University Press, Cambridge, UK)

Peraiah, A., & Srinivasa Rao, M. 1998, A&AS, 132, 45 (Paper I)

Sobolev, V. V. 1963, A Treatise on Radiative Transfer (Van Nostrand, New York)

Srinivasa Rao, M., & Peraiah, A. 2000, A&AS, 145, 525 (Paper II)

Vaz, L. P. R. 1985, Ap&SS, 113, 349

Wilson, R. E. 1990, ApJ, 356, 613

Wing, G. M. 1962, An introduction to Transfer Theory (John Wiley, New York)

Yu. Skul'skij, M. 1993, Soviet Astron. Lett., 19, No. 1 (Translated from Pis'ma Astron. Zh., 19 (1), 45)